EPA-600/2-77-209b
November 1977

Environmental Protection Technology Series

AMERICAN AIR FILTER KINPACTOR 10 x 56 VENTURI SCRUBBER EVALUATION

Industrial Environmental Research Laboratory
Office of Research and Development
U.S. Environmental Protection Agency
Research Triangle Park, North Carolina 27711

RESEARCH REPORTING SERIES

Research reports of the Office of Research and Development, U.S. Environmental Protection Agency, have been grouped into five series. These five broad categories were established to facilitate further development and application of environmental technology. Elimination of traditional grouping was consciously planned to foster technology transfer and a maximum interface in related fields. The five series are:

1. Environmental Health Effects Research
2. Environmental Protection Technology
3. Ecological Research
4. Environmental Monitoring
5. Socioeconomic Environmental Studies

This report has been assigned to the ENVIRONMENTAL PROTECTION TECHNOLOGY series. This series describes research performed to develop and demonstrate instrumentation, equipment, and methodology to repair or prevent environmental degradation from point and non-point sources of pollution. This work provides the new or improved technology required for the control and treatment of pollution sources to meet environmental quality standards.

EPA REVIEW NOTICE

This report has been reviewed by the U.S. Environmental Protection Agency, and approved for publication. Approval does not signify that the contents necessarily reflect the views and policy of the Agency, nor does mention of trade names or commercial products constitute endorsement or recommendation for use.

This document is available to the public through the National Technical Information Service, Springfield, Virginia 22161.

EPA-600/2-77-209b
November 1977

AMERICAN AIR FILTER KINPACTOR 10 x 56 VENTURI SCRUBBER EVALUATION

by

Seymour Calvert, Harry Barbarika, and Gary M. Monahan

Air Pollution Technology, Inc.
4901 Morena Boulevard, Suite 402
San Diego, California 92117

Contract No. 68-02-1869
ROAP No. 21ADM-029
Program Element No. 1AB012

EPA Project Officer: Dale L. Harmon

Industrial Environmental Research Laboratory
Office of Energy, Minerals, and Industry
Research Triangle Park, N.C. 27711

Prepared for

U.S. ENVIRONMENTAL PROTECTION AGENCY
Office of Research and Development
Washington, D.C. 20460

ABSTRACT

An American Air Filter Kinpactor 10 x 56 venturi scrubber operating on the emissions from a large borax fusing furnace has been evaluated. The average total efficiency was 97.5 % during the test period. The venturi was operated at a pressure drop of 110 cm W.C., using about 33 liters/s of scrubbing liquor for a gas flow rate of approximately 20 Am^3/s (43,000 CFM) at 80°C. The dust had a mass median aerodynamic diameter of about 0.8 μmA.

The collection efficiencies of particles with aerodynamic diameters between 0.3 μmA and 3 μmA were determined from size distribution data taken with cascade impactors. The efficiency data showed the venturi to be more efficient than predicted for particle sizes below 1 μmA. Particle mass augmentation by condensed water is a probable reason for the high efficiency for small particle collection. Diffusion battery data indicate the occurrence of some particle growth.

Cost data supplied by the user showed that the venturi scrubber system initially cost about $29,000/($m^3/s$) ($13.70/CFM) in 1970.

This report was submitted in partial fulfillment of Contract No. 68-02-1869 by Air Pollution Technology, Inc. under the sponsorship of the U.S. Environmental Protection Agency.

CONTENTS

FIGURES

FIGURES (continued)

TABLES

SECTION 1

INTRODUCTION

Air Pollution Technology, Inc. (A.P.T.) conducted a performance evaluation of an American Air Filter Kinpactor 10 x 56 venturi scrubber in accordance with E.P.A. Contract No. 68-02-1869, "Fine Particle Scrubber Evaluations."

The objective of the performance test was to determine fine particle collection efficiency as a function of particle size and scrubber parameters.

Simultaneous inlet and outlet particle sampling measurements were taken on the scrubber during a six day test period during August, 1976. Cascade impactors, condensation nuclei counters, and a portable diffusion battery were used to obtain total mass loadings and size distribution data. The data and results of the evaluation of the scrubber are presented in the text.

SECTION 2

SUMMARY AND CONCLUSIONS

The American Air Filter Kinpactor 10 x 56 venturi scrubber operating on the emissions from a large borax fusing furnace had an average total efficiency of 97.5 % during the testing period. The venturi was operated at a pressure drop of 110 cm W.C., using about 33 liters/s of scrubbing liquor for a gas flow rate of approximately 20 Am^3/s (43,000 ACFM) at 80°C. The dust had a mass median aerodynamic diameter of about 0.8 μmA.

The collection efficiencies of particles with aerodynamic diameters between 0.3 μmA and 3 μmA were determined from size distribution data taken with cascade impactors. The efficiency data showed the venturi to be more efficient than predicted for particle sizes below 1 μmA. Probable reasons for the higher experimental efficiency in the smaller size range of particles were collection by condensation and particle growth. Diffusion battery data support the reasoning for the higher experimental efficiency for the smaller size range. The major condensation mechanism is that of water vapor on drops which have a low vapor pressure because they contain dissolved borax ($Na_2B_4O_7$).

Cost data supplied by the user showed that the venturi scrubber system initially cost about $\$29,000/(m^3/s)$ in 1970.

SECTION 3

SOURCE AND CONTROL SYSTEM

The emission source was a large borax fusing furnace used in continuous operation. The furnace was capable of producing 2.7 x 10^5 kg per day of anhydrous borax ($Na_2B_4O_7$) from the pentahydrated form of the feed, but was not always operating at full capacity during the testing. The particulates emitted were primarily the hydrated and anhydrous forms of borax which escaped during the drying and fusing processes.

The total scrubbing system is shown in Figure 1, with the location of the sampling ports indicated. The gases from the furnace at a temperature of 1,000°C to 1,100°C are quenched by scrubbing liquor to about 80°C. The gases then enter the American Air Filter Kinpactor 10 x 56 venturi scrubber, which is shown in schematic in Figure 2. The venturi is rectangular in cross section with a throat height of 142 cm (56 inches). The throat width is automatically controlled to maintain a pressure drop of about 110 cm W.C. (43 in W.C.) across the venturi. The throat width can vary from 0.64 cm (0.25 in) to 25.4 cm (10 in). Following the venturi the gases enter a cyclone entrainment separator which is shown in Figure 3. The gas is moved through the scrubbing system by a blower which is rated at 44 Am^3/s at 84°C and 114 cm W.C. pressure differential (93,500 ACFM, 184°F, 45 in W.C.). The blower is powered by a 746 kW (1,000 HP) motor. The gases exhaust to the atmosphere through a 21 m tall, 2.13 m diameter stack.

The scrubbing liquor is recycled through a tank which is fed about 28 ℓ/s of fresh liquor or lesser amounts of fresh water. About 22 ℓ/s of concentrated liquor is pumped from the bottom of the tank so that the borax concentration of the liquor is maintained at from 10 to 15 percent.

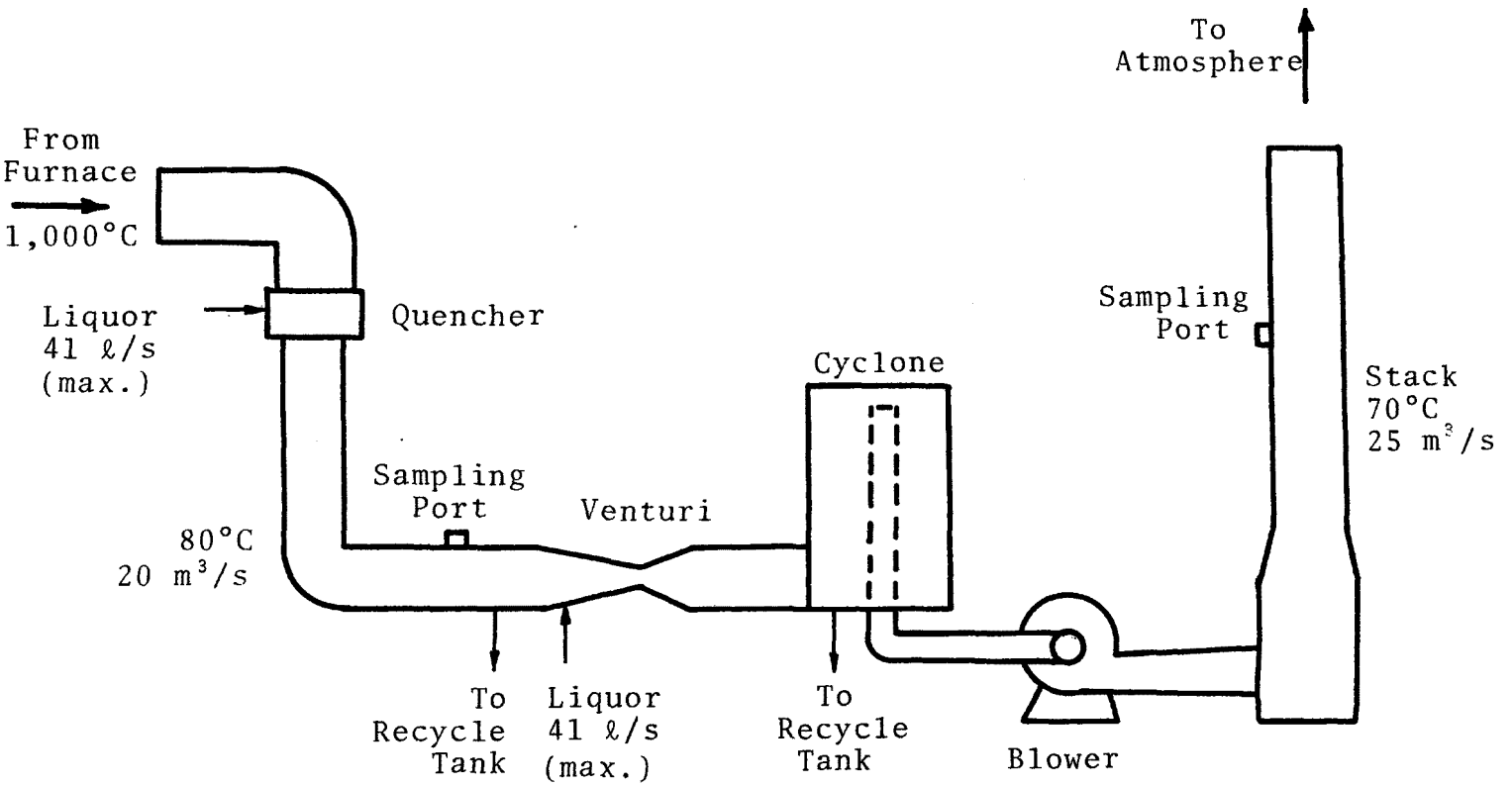

Figure 1. Schematic diagram of scrubbing system.

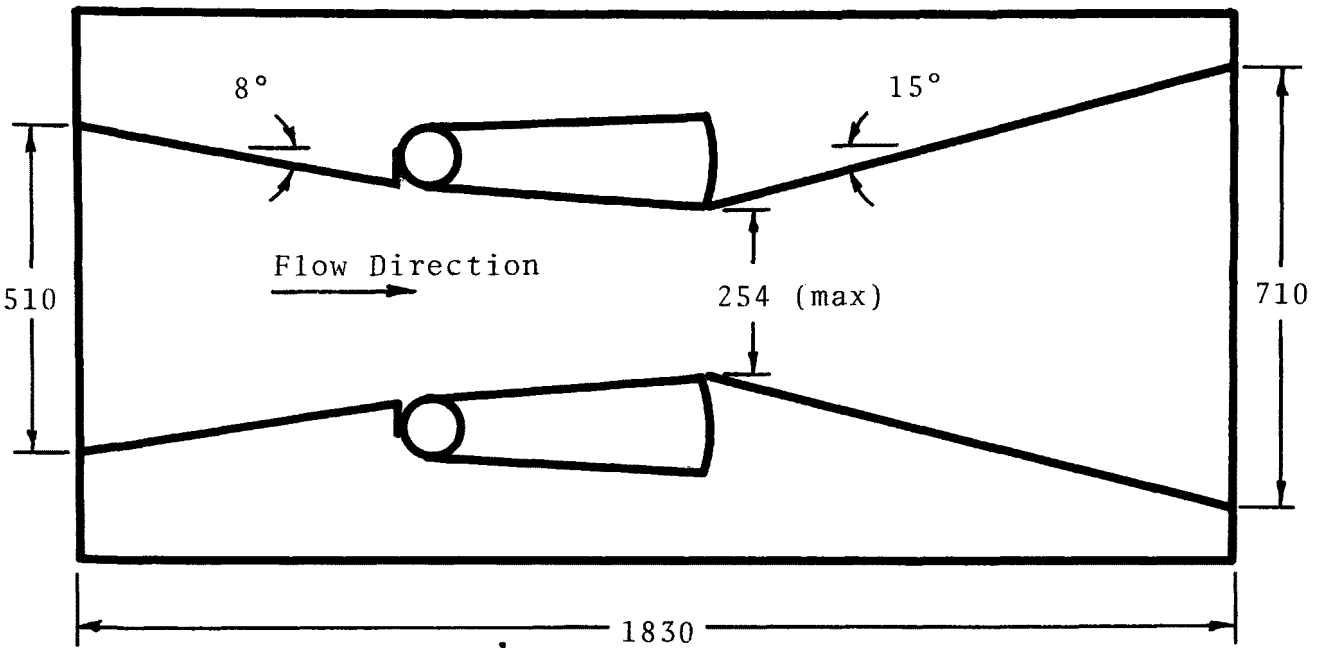

Figure 2. Schematic top view of A.A.F. Kinpactor 10 x 56, shown in fully open position (dimensions in millimeters).

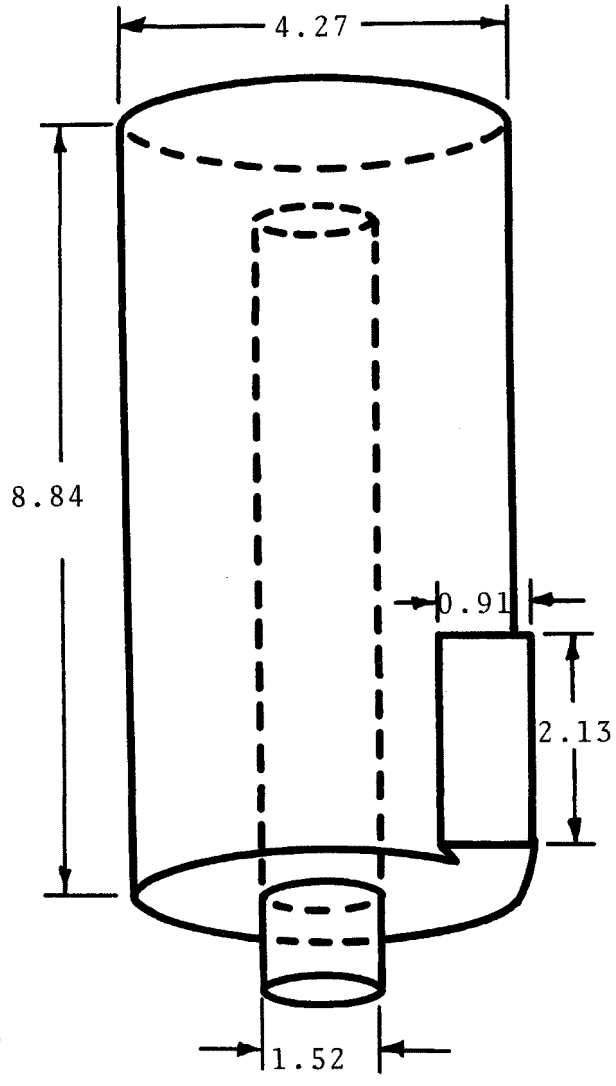

Figure 3. Schematic of cyclone entrainment separator (dimensions in meters).

SECTION 4

TEST METHOD

The performance characteristics of the American Air Filter Kinpactor 10 x 56 venturi scrubber were determined by measuring the particle size distribution and mass loading of the inlet and outlet gas simultaneously.

For the tests performed in August 1976, modified E.P.A. type sampling trains with in-stack heated University of Washington Mark III (U.W.) cascade impactors were used for particle measurements above 0.3 μmA. Figure 4 shows a schematic diagram of the modified sample train. Glass fiber filter (Gelman type AE) substrates were used in the impactors to prevent particle bounce and minimize wall losses. Low velocity impactor jet stages were used for the majority of test runs on the inlet sampling to increase the sampling time.

The Air Pollution Technology portable screen diffusion battery (A.P.T.-S.D.B.) was used for particle measurements from 0.1 μm to 0.01 μm (actual).

The A.P.T.-S.D.B. uses Brownian diffusion to accomplish the size fractionation of particles smaller than 0.1 μm. Because smaller particles diffuse more readily than larger ones, successively larger particles are captured as they proceed through the battery.

A condensation nuclei counter (C.N.C.) was used to determine the particle number concentration at several locations in the battery. From this data, the size distribution may be determined for the particles smaller than 0.1 μm. The size distribution computation was based on a calibration of the S.D.B. performed in the A.P.T. laboratory.

During an impactor run, inlet or outlet fine particle size measurements were taken with the portable diffusion battery.

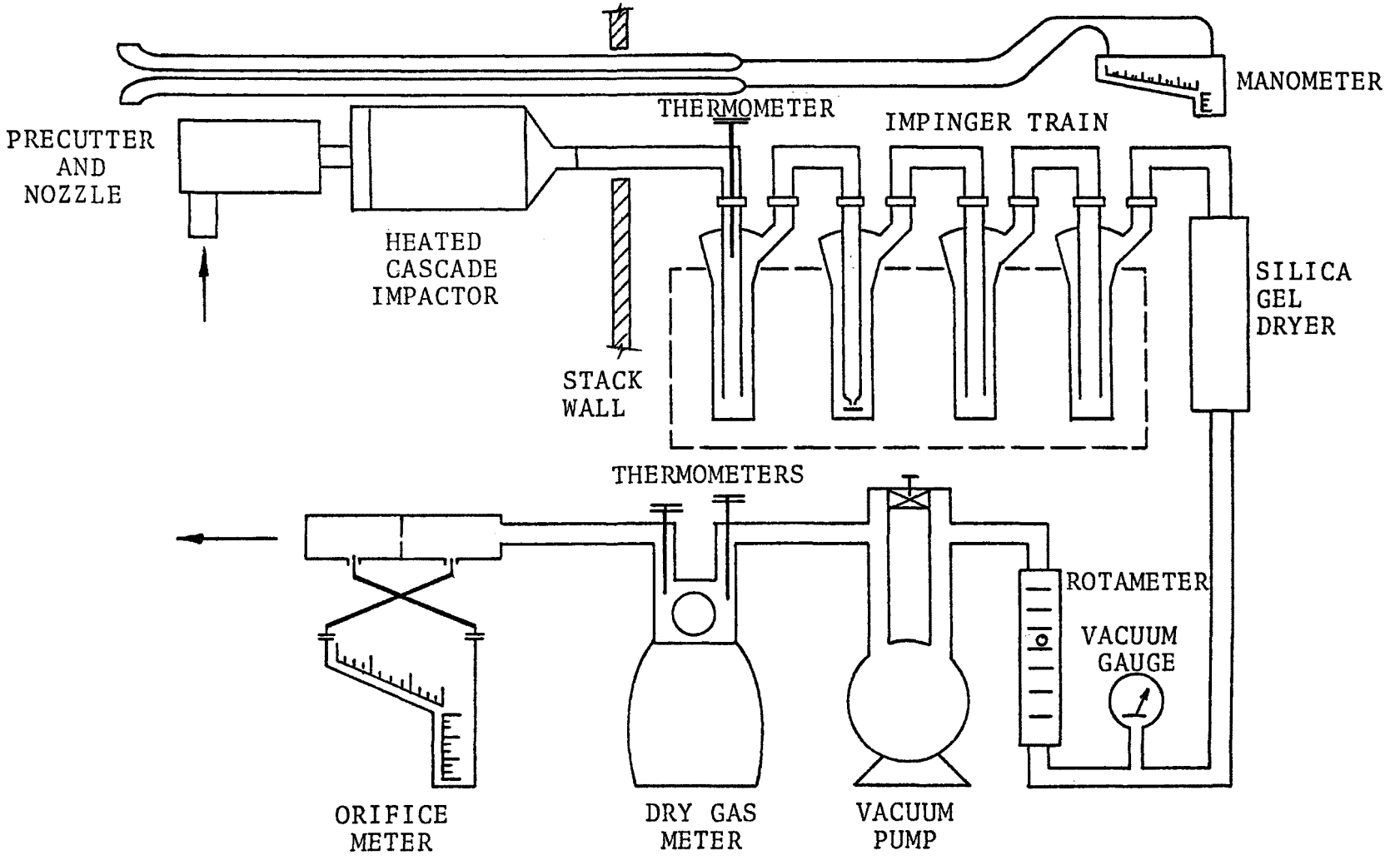

Figure 4. Modified EPA sampling train with in-stack cascade impactor

Since the system remained fairly constant during the test period, inlet and outlet S.D.B. measurements at different times were considered to approximate simultaneous sampling.

Impactor blank runs on the inlet were performed periodically to insure that the substrates did not react with the stack gases. A blank impactor run consisted of an impactor preceded by two glass fiber filters run at identical sample conditions as the actual sampling runs.

Gas flow rates for all tests were determined by means of a calibrated standard-type pitot tube along with in-stack taps for continuous wet and dry bulb temperature measurements. Velocity traverses of the inlet and outlet were performed according to the E.P.A. standards and average velocity points selected for one-point sampling. Sampling flow rates were measured with the usual E.P.A. train instruments so as to obtain isokinetic sampling. Orsat analysis of the outlet gases was also performed.

The inlet sample ports were located in the best place available, but in a relatively poor location for sampling. The inlet duct was square and 1.52 m (5 ft) on a side. The sample ports were 0.4 duct diameters downstream of a 90° bend and 1 duct diameter from the beginning of the venturi section. Twenty point velocity traverses through the center of the duct from both the top and the side were used to determine the flow rate and the location for the cascade impactor sampling. Since the flow was not well developed at the inlet sampling port, the inlet flow rate values are less reliable than the outlet flow rates.

The outlet sample ports were located in a 2.13 m (7 ft) diameter round stack, five diameters downstream of the inlet from the fan and about 4 diameters upstream of the stack exit. The velocity traverses indicated well developed flow.

SECTION 5

PROCESS CONDITIONS

Thirteen cascade impactor sampling runs were made over a period of six days. The gas conditions at the inlet and outlet sampling locations during the runs are shown in Tables 1 and 2. It is thought, from observations of the amount and consistency of the product from the fusing furnace during the period, that the conditions during runs 9 through 13 are most representative of normal conditions. The average barometric pressure during the testing period was 93.63 kN/m^2 (27.65 in Hg).

Close examination of the inlet and outlet flow rates uncovers a violation of the mass conservation law since the outlet flow rate is greater than the inlet flow rate while the inlet temperature is greater than the outlet temperature. The static pressures are practically equal. There are two explanations for this flow rate discrepancy: 1) As noted previously, the inlet flow is not well developed and thus the inlet flow rate is probably not accurate and, 2) air could be leaking into the system because of the low pressure (-110 cm W.C. gage) within the system between the venturi and the blower.

The results on the Orsat analysis of the outlet gas are presented in Table 3.

TABLE 1. INLET PROCESS CONDITIONS

Run	Temp. °C	Water Volume Percent *	Static Press. cm W.C.	Flow Rate Am^3/s (ACFM)
1	75	36	-8.3	24 (51,000)
2	108	57	-6.5	21 (45,000)
3,4,5	73	14	-6.1	16 (35,000)
6,7,8	78	23	-7.2	18 (38,000)
9,10,11	79	49	-7.5	20 (42,000)
12,13	81	41	-8.6	20 (43,000)

TABLE 2. OUTLET PROCESS CONDITIONS

Run	Temp. °C	Water Volume Percent *	Static Press. cm W.C.	Flow Rate Am^3/s (ACFM)
1	80	31	-0.5	29 (62,500)
2	73	33	-0.4	25 (54,000)
3,4,5	72	38	-0.4	25 (54,000)
6,7,8	68	28	-0.4	25 (54,000)
9,10, 11	71	23	-0.4	25 (53,000)
12,13	69	21	-0.4	25 (53,000)

* Based on wet and dry bulb temperatures

TABLE 3. OUTLET AVERAGE GAS COMPOSITION

Gas Component	Volume Percent Wet	Volume Percent Dry
N_2	60	85
O_2	6	8
CO_2	5	7
CO	0	0
H_2O	29	---
Molecular Wt.	26	29

SECTION 6

CASCADE IMPACTOR PARTICLE DATA

Particle size distribution data were obtained for the American Air Filter Kinpactor venturi scrubber as described in the Test Method section. Identical single point sampling at the average velocity location was performed at both the inlet and outlet. The sampling time of each run depended on the mass loading. The average sampling times for the inlet and outlet were nine and fifty minutes respectively.

Because of the number of very large particles in the inlet gas and the entrained water droplets at the inlet and outlet, precutters were used. The aerodynamic cut diameters of the inlet and outlet precutters were approximately 12 μmA and 4.5 μmA respectively. The inlet sampling was approximately isokinetic. However, because of the large amount of water droplets in the outlet gas, a special "rain can" had to be used on the outlet sampling nozzle. Also, the outlet sampling nozzle was oriented perpendicular to the gas flow. The velocity through the outlet nozzle was maintained at the velocity of the outlet flow at that location.

Isokinetic conditions are not crucial for sampling fine particles. For example, the error caused by sampling 4 μmA particles at a velocity 50% higher or lower than the gas stream velocity would only be 2 or 3% of the concentration.

The use of single point sampling and perpendicularly oriented nozzles is usually permissible when measuring fine particle size and concentration. The fine particles will be distributed well in the gas stream, except in cases where streams with different particle concentrations have not had sufficient time to mix. To illustrate that one-point sampling is sufficient for fine parti-

cles, we may note that Stokes stopping distance of a 3 μmA particle with an initial velocity of 15 m/sec (50 ft/sec) is about 0.04 cm (0.016 inches) and for a 1 μmA diameter particle is one-ninth of that. Since the stopping distance is the maximum that a particle can be displaced from a gas streamline by going around a right angle bend, it is apparent that fine particle distribution in the gas stream will be negligibly affected by flow direction changes.

To minimize the possibility of condensation in the impactors and to collect only the dry particles, the impactors were maintained at about 15°C above the gas stream temperature by heating blankets. The precutters were not heated.

The fact that the impactors were heated should be noted when interpreting the size distribution data. Some unpublished data taken with heated and unheated cascade impactors in a stream of wet borax particles have shown differences in the size distributions. The primary difference was that the mass median aerodynamic diameter of the borax particles collected in heated impactors was as low as 70 percent of the mass median aerodynamic diameter of the particles collected in unheated impactors. Thus, the venturi scrubber of the present system, which operates on the principle of impaction, may be experiencing larger aerodynamic size particles than the heated cascade impactor data indicate.

Data from run 3 are not included because the outlet cascade impactor stages had become wet. This happened because sampling with a parallel orientation of the outlet nozzle was tried for this run.

Particle concentration, particle size and sampled volumes for cascade impactor runs are tabulated in the Appendix in Tables A-1 through A-12. Size distributions for the impactor runs are given in Figures A-1 through A-12 located in the Appendix. The inlet and outlet size distributions both indicate a bimodal nature. The straight dashed lines drawn on Figures A-1 through A-12 represent the region of the size distributions where

log-normality may exist. The lines on the outlet distributions may approximate the lower range mode of a bimodal log-normal distribution. For want of a better ananlytic description of the size distributions, the mass mean geometric diameters and geometric standard deviations for the log-normal parameters as well as the mass median diameter (from the data points) runs are presented in Table 4.

In this report, the symbol "d_{pa}" refers to aerodynamic diameter, which is equal to the particle diameter (d_p) in microns (μm) times the square root of the particle density (ρ_p) in grams per cubic centimeter (g/cm^3) times the square root of the Cunningham slip correction factor (C'). The symbol "μmA" represents the units of aerodynamic size.

$$d_{pa} = d_p \left(\rho_p C'\right)^{1/2}, \ \mu mA \qquad (1)$$

TABLE 4. PARTICLE SIZE DISTRIBUTION SUMMARY

Run	Inlet			Outlet		
	d_{pm}	d_{pg}	σ_g	d_{pm}	d_{pg}	σ_g
	µmA	µmA		µmA	µmA	
1	0.80	0.84	2.1	0.40	0.55	2.0
2	0.94	0.99	3.3	1.1	0.78	3.2
4	--	2.3	3.7	0.32	0.32	2.6
5	0.86	0.77	2.7	--	0.22	2.9
6	--	1.9	3.3	0.33	0.41	2.1
7	0.92	0.85	4.7	--	0.20	2.8
8	0.82	0.79	3.3	0.23	0.22	3.4
9	0.66	0.55	2.7	--	0.13	3.6
10	0.86	0.83	3.3	--	0.16	3.5
11	0.76	0.69	2.7	0.25	0.25	5.2
12	0.94	1.2	3.3	--	0.16	3.6
13	0.75	0.72	3.0	--	0.19	3.5

Note: d_{pm} = mass median aerodynamic particle diameter from data

d_{pg} = log-normal geometric mass mean aerodynamic particle diameter

σ_g = log-normal geometric standard deviation

SECTION 7

DIFFUSION BATTERY DATA

Diffusion battery data were taken during the fifth and sixth days of testing. The inlet data were taken during cascade impactor runs 9, 10 and 11, while the outlet data were taken during runs 12 and 13. The average diffusion battery data particle size distribution for the inlet and outlet are shown in Figure A-13 in the Appendix.

Because of the large amount of water vapor (40% by volume) in the gas, the lenses in the condensation nuclei counter of the diffusion battery would fog when the diffusion battery was operated in the normal manner. Increased dilution did not solve the problem because the particle count would then drop below the threshold of the counter. Also, heating the diffusion battery to its maximum allowable temperature in an effort to reduce condensation on the lenses did not help.

The modification to the system that allowed data to be taken was to route the incoming source gas through a glass flask before entering the diffusion battery. Enough of the water vapor condensed in the flask so that the condensation nuclei counter did not become inoperable. Any condensation of water vapor would cause collection of submicron particles by diffusiophoresis. Thus, a fraction of the particles did not reach the diffusion battery.

Since the diffusion battery data were taken with condensation occurring within the system, the size distributions shown in Figure A-13 of the Appendix may not be accurate. However, since the configurations for taking the outlet data and the inlet data were the same and the process was constant during the testing period, the data may indicate something about the relation between the distribution of submicron particles of the inlet and outlet. The data do show that the outlet submicron particles are larger

and more monodisperse.

The data showing particle growth are only qualitative since condensation occurred within the measuring system. Mechanisms for particle growth are present in the scrubber system. These mechanisms are discussed in the section on performance comparisons.

SECTION 8

PARTICLE PENETRATIONS

Particle penetration versus particle aerodynamic diameter was calculated from the cascade impactor data. The results are shown in Figures 5 through 9 for each day of testing. Penetrations for run 1 are not shown because they are much higher than the penetrations for all the other runs, indicating anomalous behavior. Penetrations for runs of the last two days, when operations were smoothest, are quite consistent.

Because the size distributions were not log-normal all of the penetrations were calculated manually. The manual method involved visually determining the slope of the cumulative mass loading versus aerodynamic particle diameter curve, drawn from the data presented in the Appendix. The ratio of the slopes of the outlet curve to the inlet curve at a certain particle size was the penetration for that particle size.

Particle penetration based on diffusion battery data is not presented because of the inaccuracies incurred during the data acquisition. Diffusion battery data are discussed in the previous section.

The total mass loadings and overall penetrations for the runs are presented in Table 5. The total mass loading was determined from analysis of the cascade impactor data. Run 1 had anomalously high overall penetration and high flow rates which indicated that something may have been wrong with the data or that the venturi was not operating properly during that run. The average penetration for all of the runs, exclusive of run 1, was 2.5%.

As noted previously, the size distributions were obtained from analysis of heated cascade impactor data. The effect of this heating was discussed in the section on cascade impactor data.

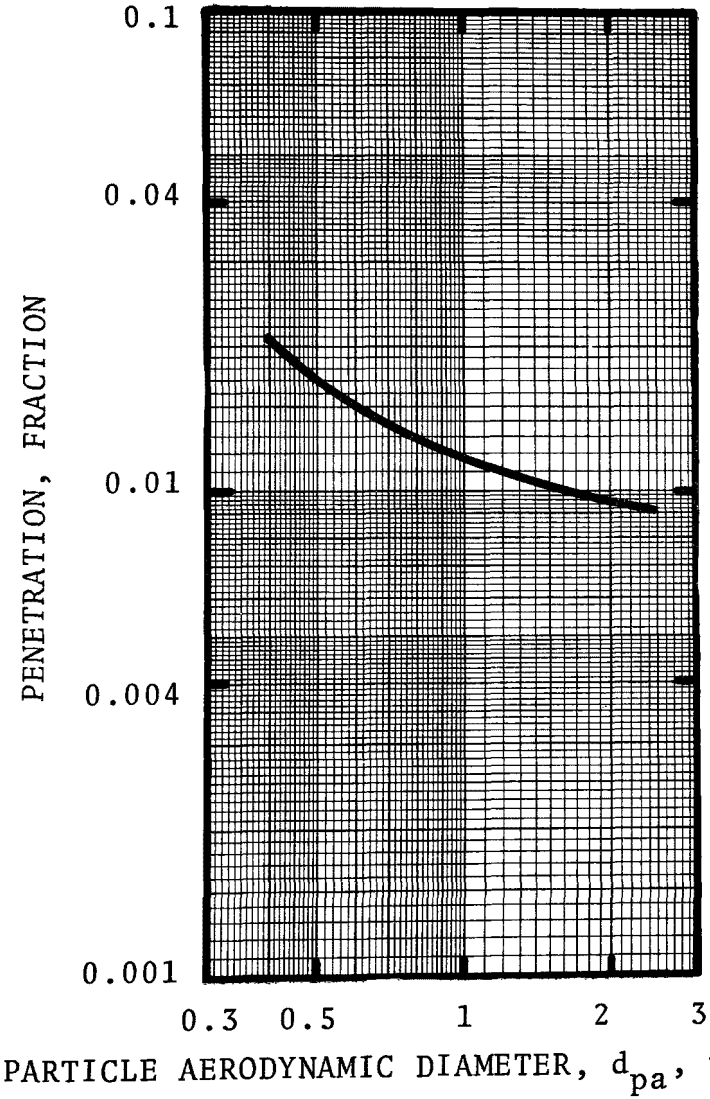

Figure 5. Particle penetration for run 2.

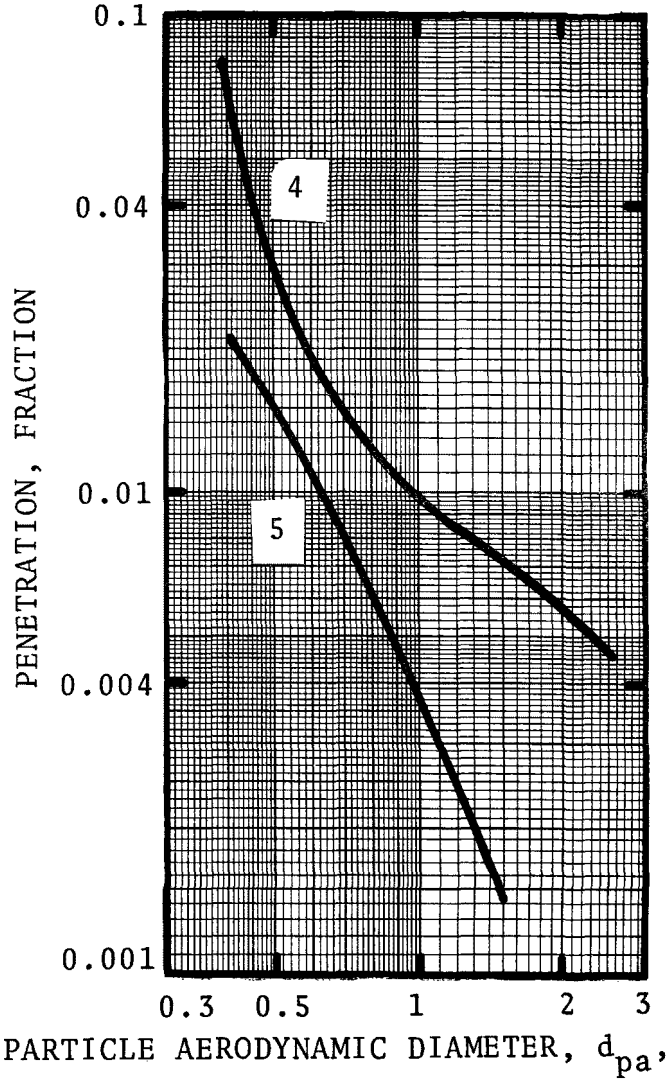

Figure 6. Particle penetration for runs 4 and 5.

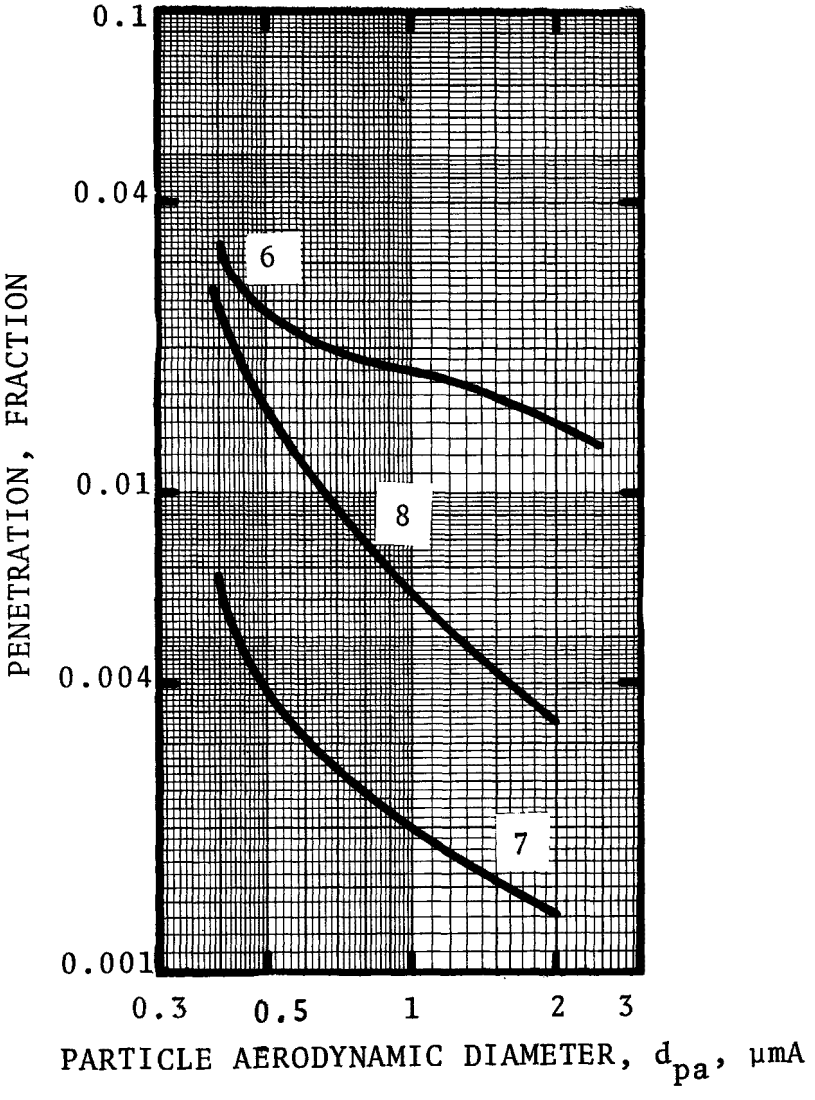

Figure 7. Particle penetration for runs 6, 7, and 8.

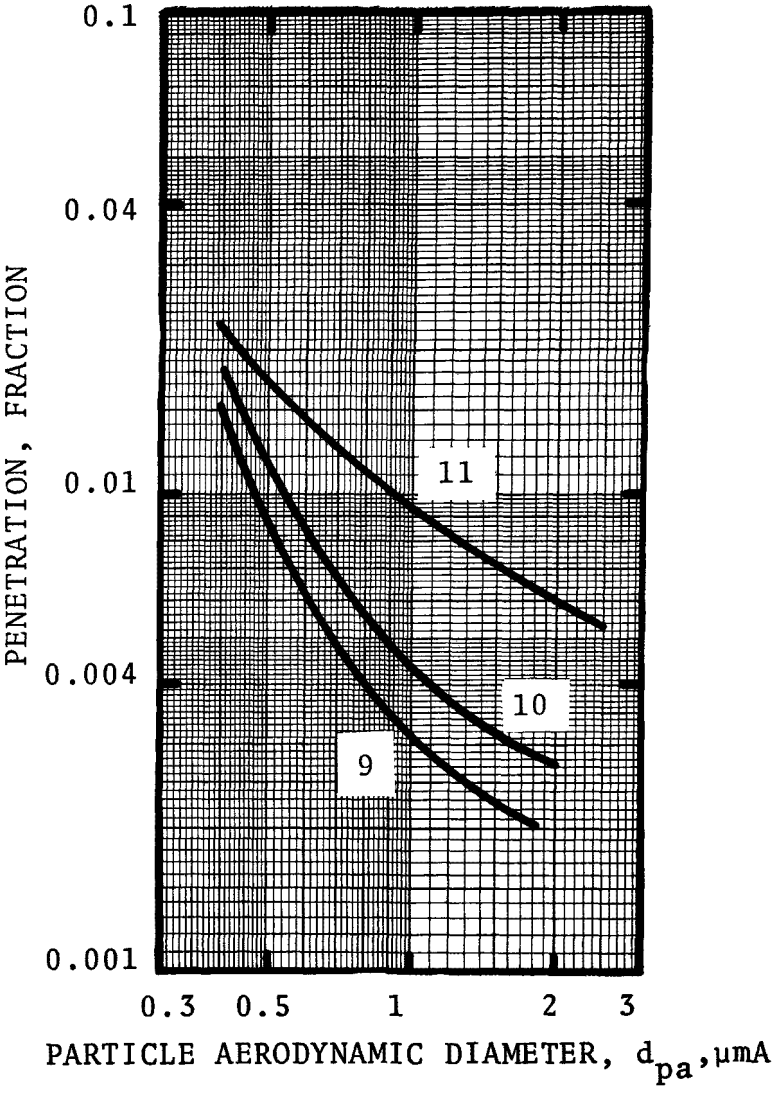

Figure 8. Particle penetration for runs 9, 10 and 11.

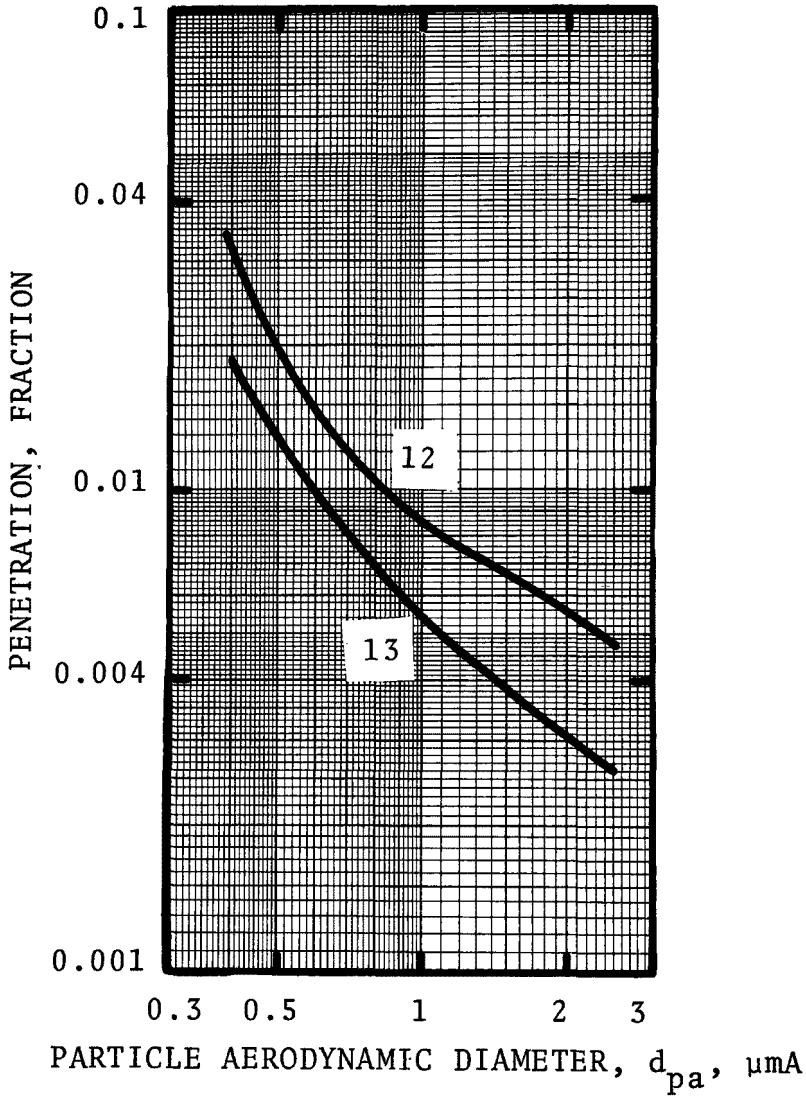

Figure 9. Particle penetrations for runs 12 and 13.

TABLE 5. MASS LOADING AND OVERALL PENETRATION

Run	Inlet Mass Loading mg/DNm^3	Outlet Mass Loading mg/DNm^3	Penetration %
1	332	40.4	12.2
2	653	18.3	2.8
4	1,150	42.1	3.7
5	841	11.0	1.3
6	690	21.9	3.2
7	2,310	18.4	0.8
8	882	20.5	2.3
9	829	22.7	2.7
10	1,040	19.3	1.9
11	863	31.0	3.6
12	1,210	36.9	3.0
13	1,000	27.3	2.7

SECTION 9

OPACITY

Opacity for the outlet stack of the American Air Filter Kinpactor 10 x 56 venturi scrubber was determined by personnel trained and certified by the California Air Resources Board. Readings were made hourly during the testing periods. The opacity determinations were made somewhat difficult by the presence of steam condensation in the plume and the proximity of other stacks emitting similar particulates.

Table 6 presents the daily average opacity readings.

TABLE 6. OPACITY

Date	Runs	Average Opacity, %	Average Outlet Loading, mg/m^3
8/19/76	2	10-15	9
8/20/76	3-5	15	12
8/21/76	6-8	20	11
8/22/76	9-11	15-20	14
8/23/76	12,13	20	19

SECTION 10

ECONOMICS

Data for the initial costs of the venturi-cyclone scrubbing system, purchased in 1970, were supplied by the user:

Approximate scrubber purchase cost	$200,000
Scrubber auxiliaries:	
1. Fans, motors, etc.	30,000
2. Ducting	47,000
3. Liquid and solid handling and treatment	50,000
4. Instrumentation	45,000
5. Electrical material	36,000
Scrubber installation:	
1. Site preparation	108,000
2. Installation	100,000
3. Start-up and modification	51,000
4. Engineering	63,000
Total Initial Cost -	$730,000

The operating costs were not available. However, the power costs can be estimated. The major power user is the large blower. The blower is powered by a 746 kW (1,000 HP) motor. At $0.03 per kW-hour the fan would cost $22 per hour, or $537 per day.

SECTION 11

OPERATING PROBLEMS

The primary operating problems with the system are the plugging of nozzles and piping and scale build-up in the system. These problems are all caused by calcium carbonate and sulfate deposits. The local water is very hard and the feed to the fusing furnaces may also contain these mineral impurities. To combat this problem special reamer nozzles have to be used and the system has to be shut down periodically to chip away the built-up scale.

Although a large amount of entrained water was carried-over from the entrainment separator through the fan, and out the stack, it was not considered a problem by operating personnel.

SECTION 12

PERFORMANCE COMPARISON

The performance of venturi-type scrubbers has been modeled extensively. The most recent survey and model* are presented in the Appendix and used here.

The scrubber parameters are known or estimated as follows:

Pressure drop	110 cm W.C.
Gas flow rate	20 Am^3/s
Liquid flow rate	0.033 m^3/s (Q_L/Q_G=0.0017)
Maximum throat area	0.361 m^2
Minimum throat velocity	69 m/s
Gas temperature	75°C
Gas density	0.79 kg/m^3
Gas viscosity	1.6×10^{-5} kg/m-s
Liquid density	1,000 kg/m^3

The gas flow rate chosen was based on outlet flow rate for runs 12 and 13 and the liquid flow rate was taken at 80 percent of the stated flow rate since it is believed that because of plugging the maximum rate was not maintained.

From the known pressure drop and a value of 0.8 for the recovery factor in the pressure equation, the following are derived:

Throat gas velocity	89 m/s
Throat area	0.28 m^2
Liquid drop diameter	0.0104 cm

Using the equations presented in Appendix B a predicted penetration versus particle aerodynamic diameter curve was con-

*Calvert, S., S. Yung and H.F. Barbarika, "Venturi Scrubber Performance Model," A.P.T., Inc., San Diego, CA, EPA Contract #68-02-1328, Task No. 13, July 1976.

structed. This curve is the "prediction" curve on Figure 10.

In order to compare the model with experiment a few important factors need to be noted:

1. Heated impactors - As explained previously the inlet and outlet size distributions were determined using heated cascade impactors. Based on previous experience it was expected that the mass median diameters of the actual wet borax particle size distributions were up to 1.5 times the sizes measured in the heated impactors. The high solubility of borax was the primary reason for the difference. Thus the venturi was collecting larger particles than those measured in the heated impactor. In order to compare the experimental results with the prediction it is necessary to plot experimental penetration against the actual (wet) particle size rather than the dried particle size. This correction causes the measured penetration curve in Figure 10 to shift toward larger particle diameters.

2. System leaks - The actual scrubber penetrations could also be different from those based on the impactor data because of dilution of the outlet by air leaks into the system, which probably did occur. Dilution of the outlet stream would cause the actual penetrations to be greater than those measured by a factor equal to the dilution factor. The outlet concentration may have been diluted as much as 25%. The dashed line on Figure 10 includes the effects of 25% dilution and 1.5 times particle growth on measured data.

3. Collection mechanism - The model for ventrui performance assumes particle collection by inertial impaction on drops in the throat region of the venturi. This model does not account for forces other than inertia which can effect submicron particle collection. Thus, in the region below about 0.5 μmA the predicted penetration and the experimental penetration are expected to differ.

Another important phenomenon is the collection of particles of all sizes due to solution induced condensation. Borax ($Na_2B_4O_7$) is highly soluble in water. If the scrubber liquor became more concentrated than would be in equilibrium with the vapor, it is

conceivable that particles could be swept toward the liquid as water vapor moves to condense on it. The liquid drops which contain dissolved borax have a reduced vapor pressure which induces the condensation which causes the growth in particle size manifested in the differences between wet and dry particle sizes.

Some of this dissolution and condensation will have occurred in the quench section upstream of the venturi. However, because of the large amount of liquid injected at the venturi these mechanisms may still be causing particle collection and growth downstream of the venturi. Growth or collection of the submicron particles after the inlet sampling point, either before or after the venturi would explain some of the differences between the predicted and the experimental penetrations.

Condensation can also occur when the vapor pressure of the water is reduced because it is at a lower temperature than the adiabatic saturation temperature of the gas. This cause of condensation was not significant here because there was very little cooling of the scrubber liquor.

4. Sensitivity of prediction to L/G ratio - The predicted curve is very sensitive to the liquid to gas volume flow rate ratio (L/G) for particle diameters above 1.0 μmA. A 25% decrease in the L/G ratio would cause the prediction to agree closely with the data. Since neither the inlet gas flow rate nor the liquid flow rate are known precisely, it is possible that the actual L/G ratio was lower than the value used in the prediction.

5. Entrainment - The carry-over from the cyclone was so heavy that precutters had to be used on the outlet sampling probe. It was possible that some smaller entrainment drops, containing dissolved borax, penetrated the precutters or were shattered in the precutters and were collected in the heated impactors. Since the venturi model assumed that no entrainment carry-over occurred, the actual penetrations would be greater than the model prediction, as seen in Figure 10.

These five factors help explain the differences between the

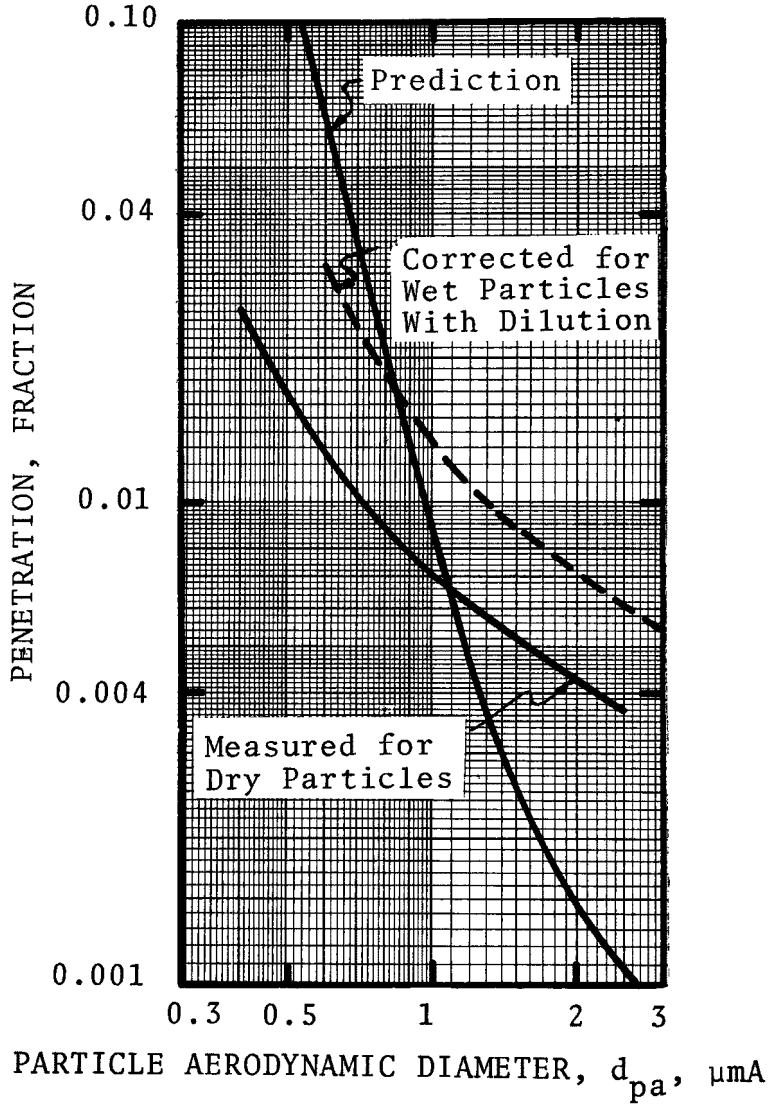

Figure 10. Particle penetration for average of runs 12 and 13 compared to prediction.

model prediction and the data. The many factors and uncertainties involved are enough to preclude any judgment of the accuracy of the model.

APPENDIX A

SIZE DISTRIBUTION DATA

TABLE A-1. INLET AND OUTLET SAMPLE PARTICLE DATA FOR RUN # 1

IMPACTOR STAGE NUMBER	INLET		OUTLET	
	M_{cum} (mg/DNm^3)	d_{pc} (µmA)	M_{cum} (mg/DNm^3)	d_{pc} (µmA)
Precutter	332	*	40.4	*
1	312	35.8	37.3	16.1
2	273	3.06	36.6	7.06
3	273	1.75	35.9	2.73
4	263	0.97	34.7	1.38
5	228	0.58	33.7	0.79
6	74.4	0.32	31.8	0.44
7	39.7	0.19	23.9	0.25
Filter	39.7		4.45	
Sample Volume (DNm^3)	0.020		0.584	

TABLE A-2. INLET AND OUTLET SAMPLE PARTICLE DATA FOR RUN #2

IMPACTOR STAGE NUMBER	INLET		OUTLET	
	M_{cum} (mg/DNm^3)	d_{pc} (µmA)	M_{cum} (mg/DNm^3)	d_{pc} (µmA)
Precutter	653		18.3	
1	458	30.0	14.3	16.7
2	458	2.57	11.6	7.31
3	447	1.47	10.7	2.83
4	422	0.81	10.4	1.43
5	284	0.49	9.56	0.82
6	165	0.27	8.42	0.45
7	85.2	0.16	6.99	0.26
Filter	45.4		3.00	
Sample Volume (DNm^3)	0.053		0.701	

* The inlet and outlet d_{pc}'s for the precutters averaged approximately 12 µmA and 4.5 µmA respectively for all runs.

TABLE A-3. INLET AND OUTLET SAMPLE PARTICLE DATA FOR RUN #4

IMPACTOR STAGE NUMBER	INLET		OUTLET	
	M_{cum} (mg/DNm^3)	d_{pc} (µmA)	M_{cum} (mg/DNm^3)	d_{pc} (µmA)
Precutter	1509		42.1	
1	524	44.3	38.3	17.2
2	519	3.79	32.7	7.51
3	498	2.17	31.9	2.91
4	461	1.20	31.7	1.47
5	360	0.72	30.3	0.84
6	218	0.40	29.6	0.46
7	113	0.23	27.5	0.27
Filter	46.1		18.2	
Sample Volume (DNm^3)	0.024		0.788	

TABLE A-4. INLET AND OUTLET SAMPLE PARTICLE DATA FOR RUN #5

IMPACTOR STAGE NUMBER	INLET		OUTLET	
	M_{cum} (mg/DNm^3)	d_{pc} (µmA)	M_{cum} (mg/DNm^3)	d_{pc} (µmA)
Precutter	841		11.0	
1	714	41.6	10.0	16.1
2	714	3.56	10.0	7.04
3	708	2.04	10.0	2.72
4	692	1.12	10.0	1.37
5	602	0.68	10.0	0.79
6	320	0.37	9.63	0.43
7	181	0.22	8.23	0.25
Filter	107		5.83	
Sample Volume (DNm^3)	0.019		0.789	

TABLE A-5. INLET AND OUTLET SAMPLE PARTICLE DATA FOR RUN #6

IMPACTOR STAGE NUMBER	INLET		OUTLET	
	M_{cum} (mg/DNm^3)	d_{pc} (μmA)	M_{cum} (mg/DNm^3)	d_{pc} (μmA)
Precutter	691		21.9	
1	417	38.8	20.0	14.7
2	293	3.32	18.9	6.42
3	293	1.90	18.2	2.48
4	283	1.05	17.4	1.25
5	233	0.63	16.7	0.72
6	159	0.35	15.3	0.40
7	34.8	0.20	13.3	0.23
Filter	24.8		4.58	
Sample Volume (DNm^3)	0.020		0.873	

TABLE A-6. INLET AND OUTLET SAMPLE PARTICLE DATA FOR RUN #7

IMPACTOR STAGE NUMBER	INLET		OUTLET	
	M_{cum} (mg/DNm^3)	d_{pc} (μmA)	M_{cum} (mg/DNm^3)	d_{pc} (μmA)
Precutter	2310		18.4	
1	2040	40.8	17.9	15.1
2	1910	3.49	17.3	6.59
3	1820	2.00	17.0	2.55
4	1720	1.10	16.3	1.29
5	1420	0.67	15.7	0.74
6	811	0.37	14.7	0.41
7	678	0.21	13.8	0.23
Filter	506		10.0	
Sample Volume (DNm^3)	0.010		0.767	

TABLE A-7. INLET AND OUTLET SAMPLE PARTICLE DATA FOR RUN #8

IMPACTOR STAGE NUMBER	INLET		OUTLET	
	M_{cum} (mg/DNm^3)	d_{pc} (μmA)	M_{cum} (mg/DNm^3)	d_{pc} (μmA)
Precutter	882		20.5	
1	821	40.8	18.5	14.6
2	787	3.49	18.5	6.41
3	749	2.00	18.5	2.48
4	710	1.10	18.5	1.25
5	621	0.67	18.0	0.72
6	338	0.37	16.9	0.40
7	227	0.21	14.4	0.23
Filter	128		10.3	
Sample Volume (DNm^3)	0.018		0.390	

TABLE A-8. INLET AND OUTLET SAMPLE PARTICLE DATA FOR RUN #9

IMPACTOR STAGE NUMBER	INLET		OUTLET	
	M_{cum} (mg/DNm^3)	d_{pc} (μmA)	M_{cum} (mg/DNm^3)	d_{pc} (μmA)
Precutter	829		22.7	
1	796	32.7	21.7	14.2
2	784	2.80	21.6	6.23
3	778	1.61	21.3	2.41
4	739	0.89	21.1	1.22
5	596	0.53	20.6	0.70
6	332	0.29	20.4	0.38
7	183	0.17	18.8	0.22
Filter	129		14.8	
Sample Volume (DNm^3)	0.033		0.695	

TABLE A-9. INLET AND OUTLET SAMPLE PARTICLE DATA FOR RUN #10

IMPACTOR STAGE NUMBER	INLET		OUTLET	
	M_{cum} (mg/DNm³)	d_{pc} (μmA)	M_{cum} (mg/DNm³)	d_{pc} (μmA)
Precutter	1040		19.3	
1	885	32.4	18.7	14.4
2	885	2.77	18.7	6.32
3	859	1.59	18.7	2.44
4	792	0.88	18.7	1.23
5	549	0.53	18.3	0.71
6	305	0.29	17.2	0.39
7	189	0.17	14.8	0.22
Filter	116		11.5	
Sample Volume (DNm³)	0.034		0.948	

TABLE A-10. INLET AND OUTLET SAMPLE PARTICLE DATA FOR RUN #11

IMPACTOR STAGE NUMBER	INLET		OUTLET	
	M_{cum} (mg/DNm³)	d_{pc} (μmA)	M_{cum} (mg/DNm³)	d_{pc} (μmA)
Precutter	863		31.0	
1	771	31.8	27.6	14.5
2	771	2.72	27.0	6.35
3	766	1.56	26.3	2.46
4	735	0.86	25.3	1.24
5	500	0.52	24.2	0.71
6	273	0.29	22.5	0.39
7	150	0.17	19.3	0.23
Filter	99.1		14.5	
Sample Volume (DNm³)	0.041		0.928	

TABLE A-11. INLET AND OUTLET SAMPLE PARTICLE DATA FOR RUN #12

IMPACTOR STAGE NUMBER	INLET		OUTLET	
	M_{cum} (mg/DNm³)	d_{pc} (μmA)	M_{cum} (mg/DNm³)	d_{pc} (μmA)
Precutter	1210		36.9	
1	912	35.8	36.0	14.9
2	898	3.06	35.5	6.52
3	875	1.76	33.8	2.52
4	812	0.97	32.8	1.27
5	647	0.58	32.0	1.73
6	296	0.32	30.6	0.40
7	155	0.19	28.0	0.23
Filter	91.2		22.4	
Sample Volume (DNm³)	0.022		0.903	

TABLE A-12. INLET AND OUTLET SAMPLE PARTICLE DATA FOR RUN #13

IMPACTOR STAGE NUMBER	INLET		OUTLET	
	M_{cum} (mg/DNm³)	d_{pc} (μmA)	M_{cum} (mg/DNm³)	d_{pc} (μmA)
Precutter	1000		27.3	
1	912	35.8	25.7	14.5
2	905	3.06	25.5	6.34
3	883	1.76	25.2	2.45
4	832	0.97	24.2	1.24
5	647	0.58	23.2	0.71
6	371	0.32	22.1	0.39
7	207	0.19	19.5	0.23
Filter	134		15.2	
Sample Volume (DNm³)	0.028		0.612	

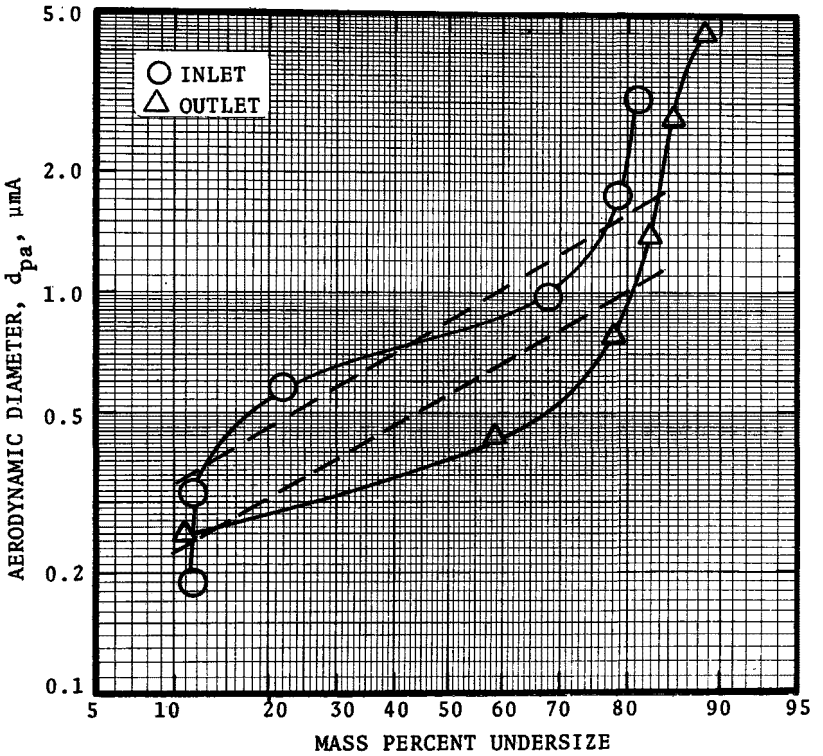

Figure A-1. Inlet and outlet size distribution for run #1.

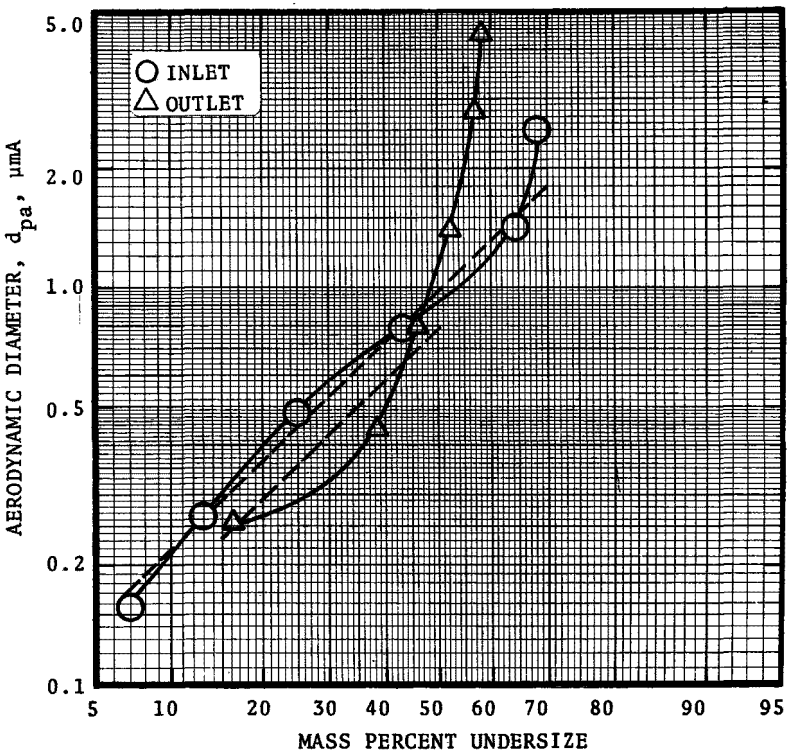

Figure A-2. Inlet and outlet size distribution for Run #2.

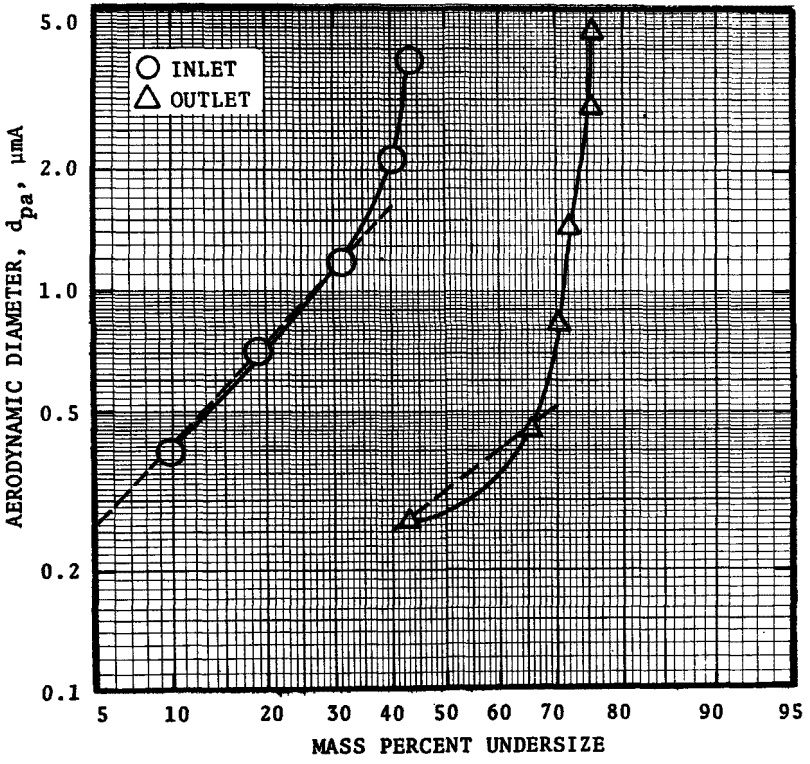

Figure A-3. Inlet and outlet size distribution for run #4.

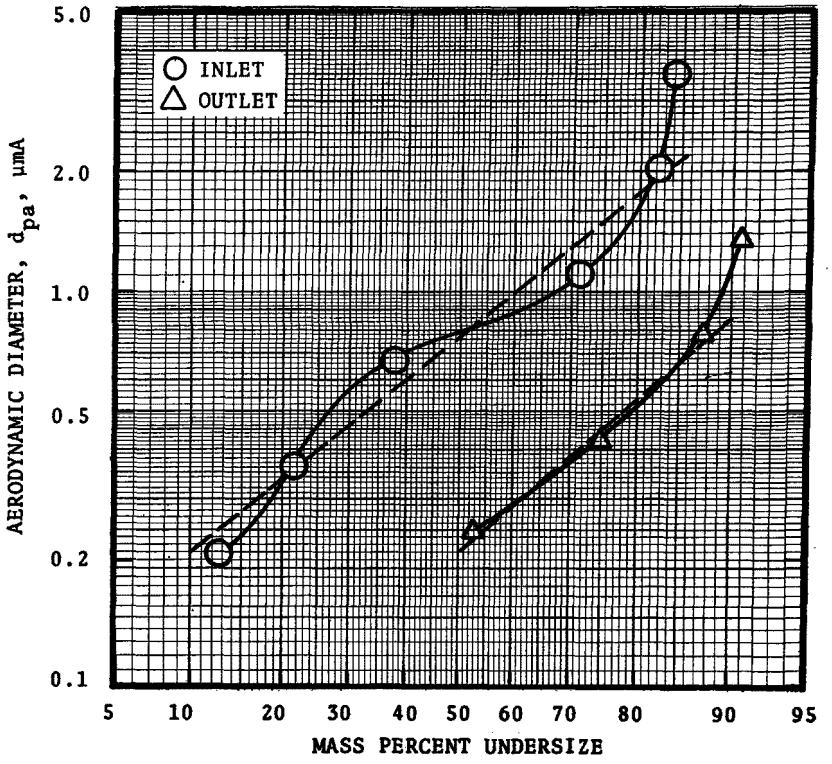

Figure A-4. Inlet and outlet size distribution for run #5.

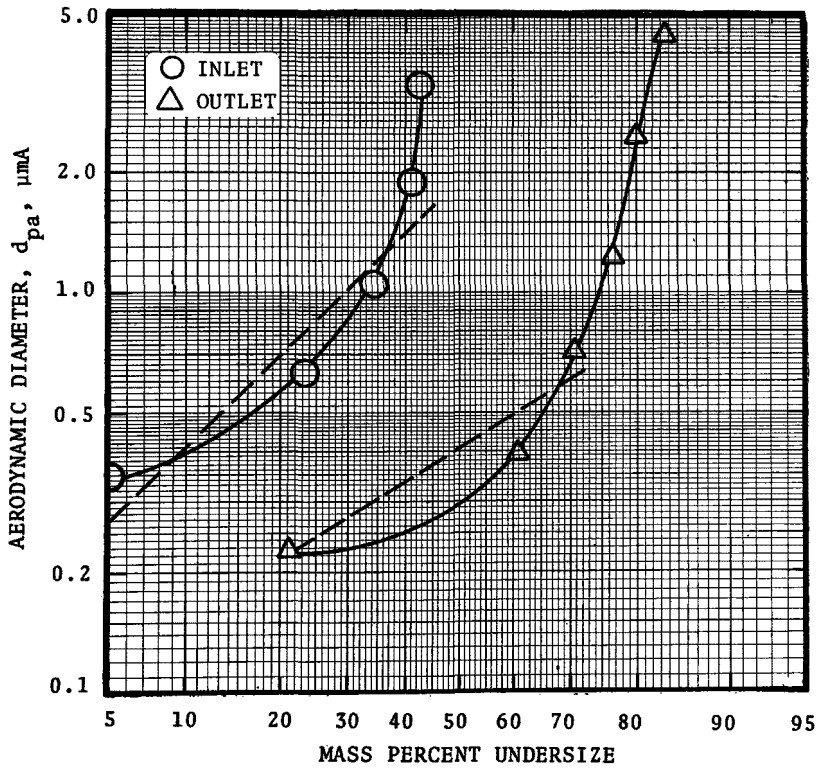

Figure A-5. Inlet and outlet size distribution for run #6.

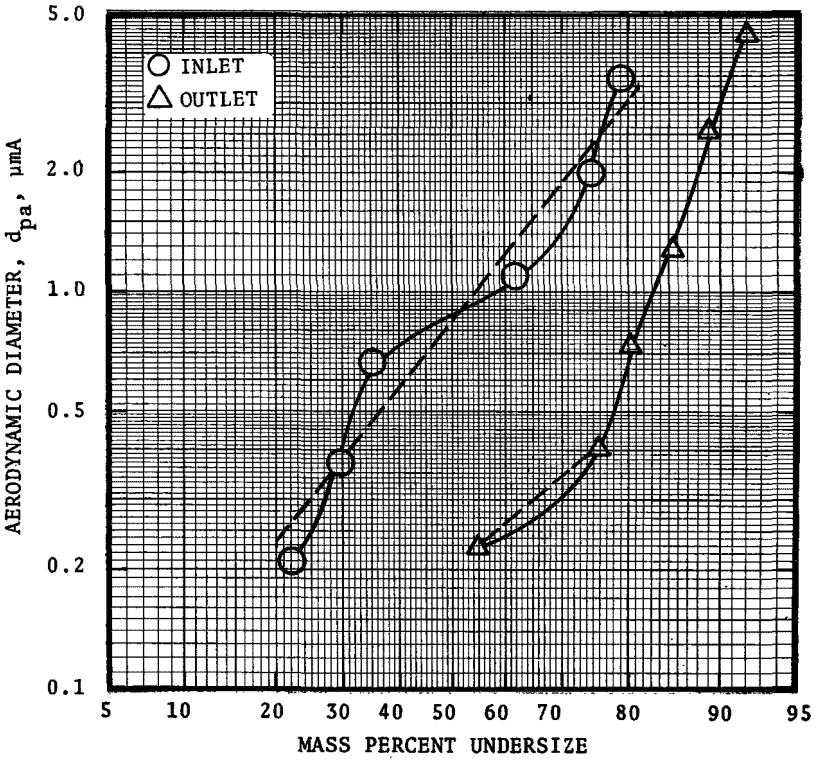

Figure A-6. Inlet and outlet size distribution for run #7.

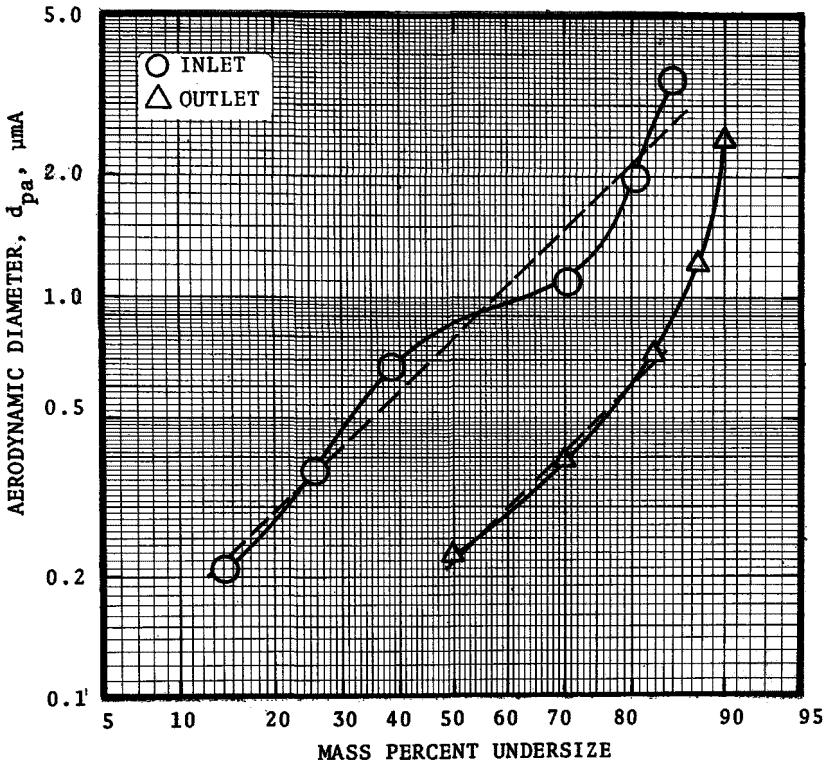

Figure A-7. Inlet and outlet size distribution for run #8.

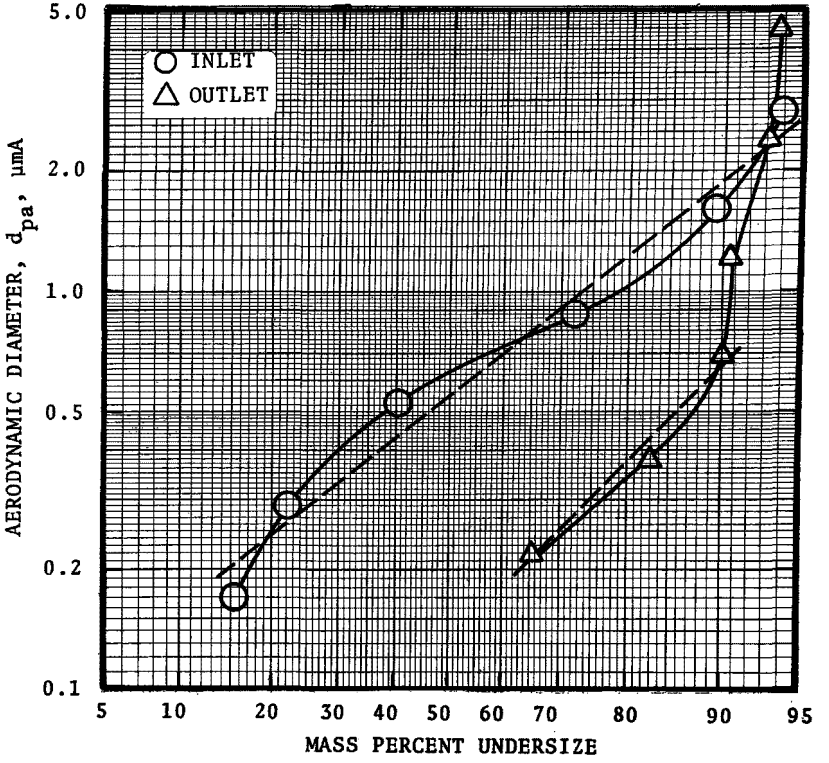

Figure A-8. Inlet and outlet size distribution for run #9.

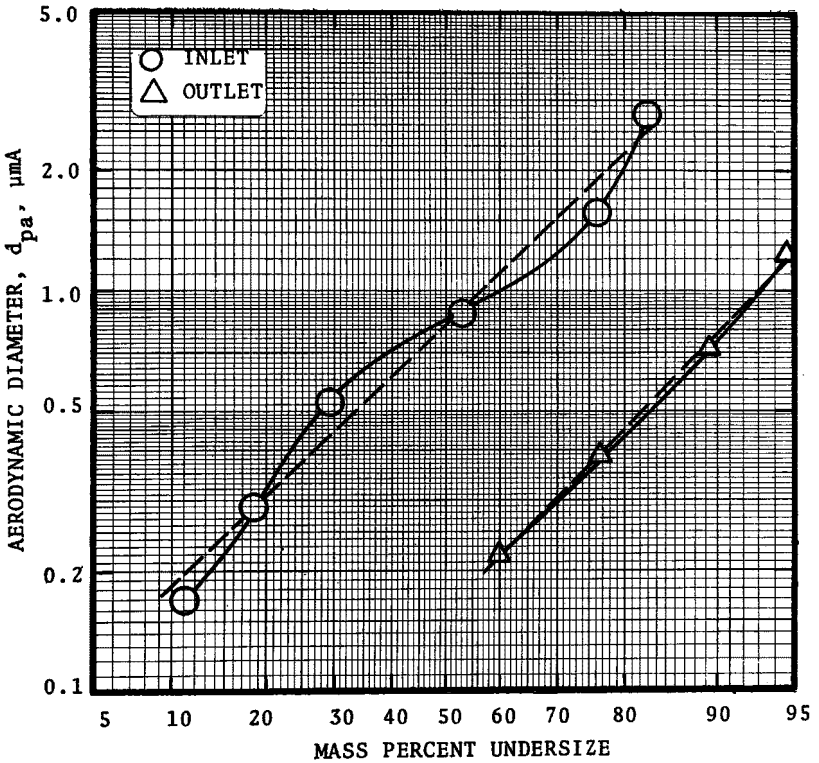

Figure A-9. Inlet and outlet size distribution for run #10.

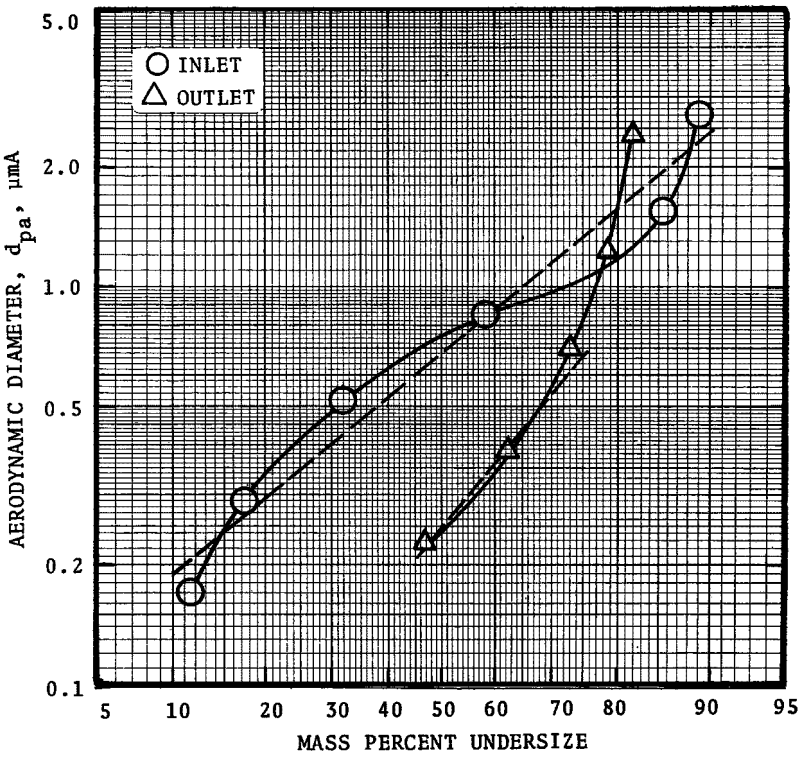

Figure A-10. Inlet and outlet size distribution for run #11.

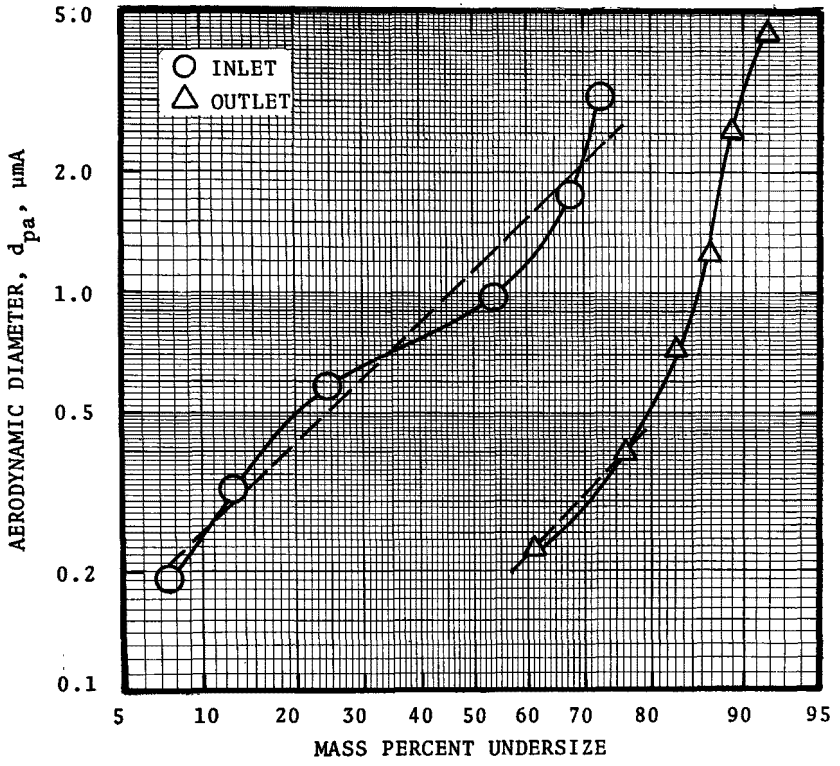

Figure A-11. Inlet and outlet size distribution for run #12.

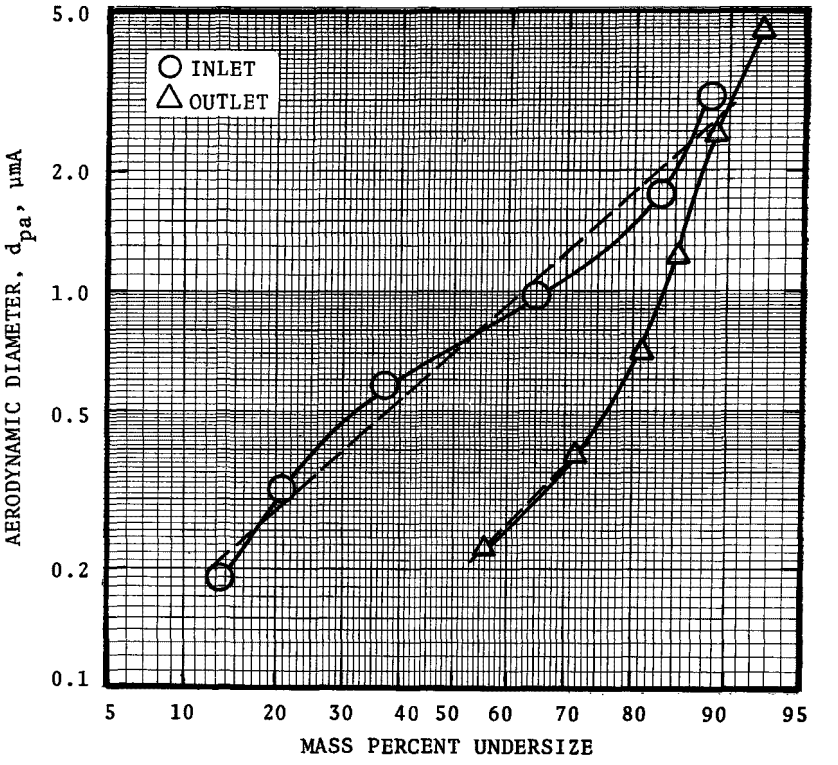

Figure A-12. Inlet and outlet size distribution for run #13.

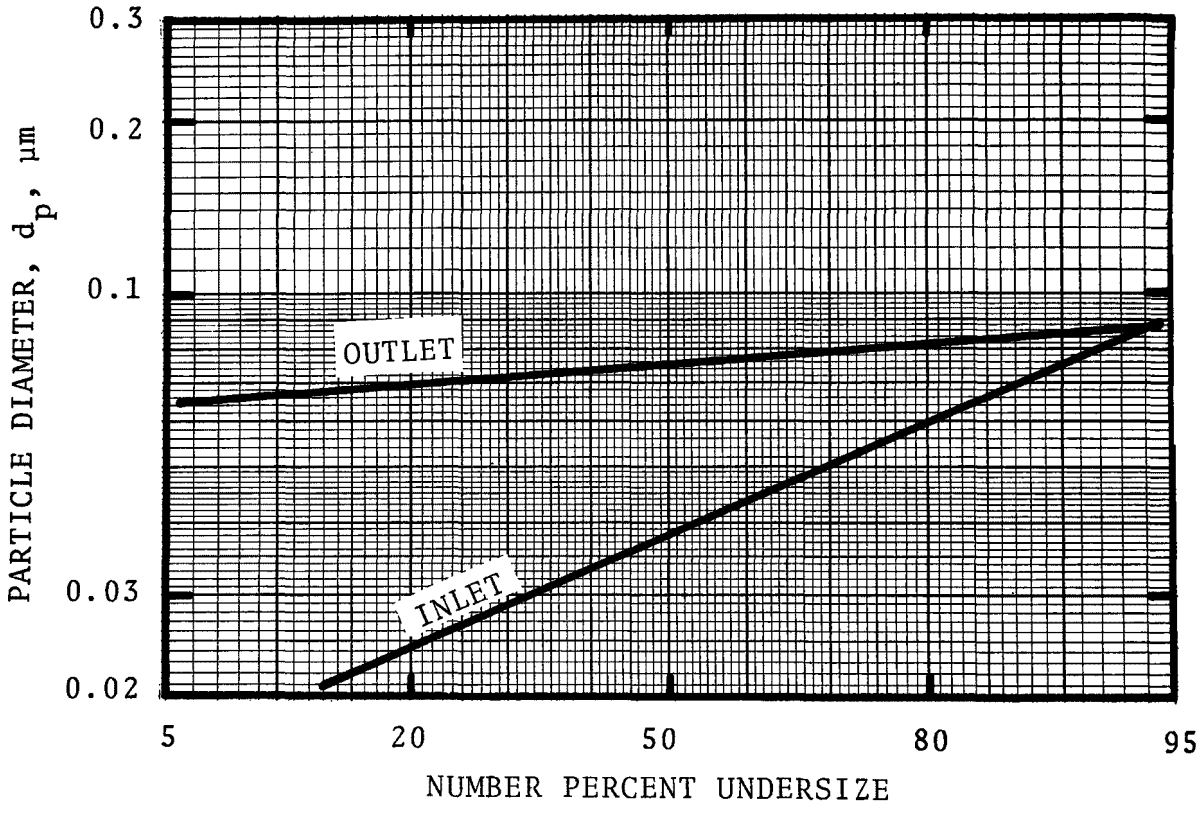

Figure A-13. Size distributions from diffusion battery data.

APPENDIX B

VENTURI SCRUBBER PERFORMANCE MODEL

VENTURI SCRUBBER PERFORMANCE MODEL

Calvert, et al., 1976 have performed a literature review and evaluation of all available venturi scrubber performance models. Their conclusions and recommended performance model are presented below.

(1) Even though each investigator presented a different equation for the prediction of particle collection in a venturi scrubber, most of these equations can be reduced to the same basic model, i.e.,

$$-\ln Pt\ (d_p) = \int_o^z \frac{3\ u_r\ Q_w\ \eta}{2\ u_G\ (u_G - u_r)\ d_d}\ dz \qquad (B\text{-}1)$$

where $Pt(d_p)$ = penetration for particles with diameter d_p, fraction

u_r = relative velocity between dust and drop, cm/sec

u_G = gas velocity, cm/sec

d_d = drop diameter, cm

η = single drop collection efficiency, fraction

Q_w = liquid volumetric flow rate, cm^3/sec

z = length, cm

(2) A generalized method for applying equation B-1 to predict particle collection in a venturi was developed.

(3) Particle collection predicted by equation B-1 agrees satisfactorily with performance data.

(4) Most of the particle collection occurs in the venturi throat. The solution to equation B-1 for the venturi throat, using the inertial collection efficiency correlation, and assuming a zero initial drop velocity, is

$$\frac{\ln Pt(d_p)}{B} = \frac{1}{K_{po}\left(1-u_d^*\right)+ 0.7}\left[4\,K_{po}\left(1-u_d^*\right)^{1.5} + 4.2\left(1-u_d^*\right)^{0.5}\right.$$

$$\left. - 5.02\,K_{po}^{0.5}\left(1-u_d^* + \frac{0.7}{K_{po}}\right)\tan^{-1}\left(\frac{\left(1-u_d^*\right)K_{po}}{0.7}\right)^{0.5}\right]$$

$$- \frac{1}{K_{po} + 0.7}\left[4\,K_{po} + 4.2 - 5.02\,K_{po}^{0.5}\left(1 + \frac{0.7}{K_{po}}\right)\tan^{-1}\left(\frac{K_{po}}{0.7}\right)^{0.5}\right] \qquad \text{(B-2)}$$

where $u_d^* = 2\left\{1 - \left(\frac{L+8}{8}\right)^2 + \left(\frac{L+8}{8}\right)\left[\left(\frac{L+8}{8}\right)^2 - 1\right]^{0.5}\right\}$

$Pt(d_p)$ = penetration for particles with diameter d_p, fraction

$B = \left(\frac{Q_L}{Q_G}\right)\left(\frac{\rho_L}{\rho_G}\right)\frac{1}{C_{Do}}$

Q_L = volumetric liquid flow rate, cm^3/sec

ρ_L = liquid density, g/cm^3

ρ_G = gas density, g/cm^3

C_{Do} = drag coefficient obtained from the "standard curve"

u_d^* = dimensionless drop velocity

$= \frac{u_d}{u_{Gt}}$

u_d = drop velocity, cm/sec

u_{Gt} = gas velocity in the throat, cm/sec

K_{po} = inertial parameter based on throat velocity

$= \frac{C'\,d_p^2\,\rho_p\,u_{Gt}}{9\,\mu_G\,d_d}$

C' = Cunningham slip factor
d_p = particle diameter, μm
ρ_p = particle density, g/cm³
μ_G = gas viscosity, poise
d_d = drop diameter, cm
L = dimensionless throat length

$$L = \frac{3\ \ell_t\ C_{Do}\ \rho_G}{2\ d_d\ \rho_L}$$

Equation B-2 slightly under estimates the particle collection occurring in a venturi scrubber. For most industrial venturi scrubbers, particle collection can be predicted closely by neglecting the first term in the right hand side of equation B-2.

(5) Pressure drop predictions by the modified Calvert's equation and by Boll's equation agree with experimental data. The modified Calvert's equation has the following form,

$$\Delta P = 1.03 \times 10^{-3}\ F_1\ u_{Gt}^2 \left(\frac{Q_L}{Q_G}\right) \qquad \text{(B-3)}$$

where ΔP = pressure, cm W.C.
u_{Gt} = gas velocity in the throat, cm/sec
Q_L = liquid flow rate, cm³/sec
Q_G = gas-flow rate, cm³/sec
F_1 = correction factor, dimensionless

$$F_1 = \frac{u_{de}}{u_{Gt}} = 2\left[1 - X^2 + (X^4 - X^2)^{0.5}\right]$$

$$X = \frac{3\ \ell_t C_{Do}\ \rho_G}{16\ d_d\ \rho_L} + 1$$

u_{de} = drop velocity at the exit of the throat, cm/sec

ℓ_t = throat length or distance between liquid injection point and the exit of throat, cm

d_d = drop diameter, cm

ρ_G = gas density, g/cm^3

ρ_L = liquid density, g/cm^3

C_{Do} = drag coefficient at the liquid injection point.

(6) The use of a drag coefficient from the "Standard curve" gives a better fit between model and experimental data than does Ingebo's correlation.

(7) The drop diameter can be assumed to be the Sauter mean diameter calculated from the Nukiyama-Tanasawa relation.

Reference: Calvert, S., S. Yung and H.F. Barbarika, "Venturi Scrubber Performance Model," A.P.T., Inc., EPA Contract No. 68-02-1328, Task 13, July 1976.

TECHNICAL REPORT DATA
(Please read Instructions on the reverse before completing)

1. REPORT NO.	2.	3. RECIPIENT'S ACCESSION NO.
EPA-600/2-77-209b		

4. TITLE AND SUBTITLE	5. REPORT DATE
American Air Filter Kinpactor 10 x 56 Venturi Scrubber Evaluation	November 1977
	6. PERFORMING ORGANIZATION CODE
7. AUTHOR(S)	8. PERFORMING ORGANIZATION REPORT NO.
Seymour Calvert, Harry Barbarika, and Gary M. Monahan	
9. PERFORMING ORGANIZATION NAME AND ADDRESS	10. PROGRAM ELEMENT NO.
Air Pollution Technology, Inc. 4901 Morena Boulevard, Suite 402 San Diego, California 92117	1AB012; ROAP 21ADM-029
	11. CONTRACT/GRANT NO.
	68-02-1869
12. SPONSORING AGENCY NAME AND ADDRESS	13. TYPE OF REPORT AND PERIOD COVERED
EPA, Office of Research and Development Industrial Environmental Research Laboratory Research Triangle Park, NC 27711	Final; 8/76-10/77
	14. SPONSORING AGENCY CODE
	EPA/600/13

15. SUPPLEMENTARY NOTES IERL-RTP project officer for this report is Dale L. Harmon, Mail Drop 61, 919/541-2925.

16. ABSTRACT The report gives results of an evaluation of an American Air Filter Kinpactor 10 x 56 venturi scrubber, operating on emissions from a large borax fusing furnace. Average total efficiency was 97.5% during the test period. The venturi was operated at a pressure drop of 110 cm W.C., using about 33 liters/s of scrubbing liquor for a gas flow rate of about 20 A cu m/s (43,000 CFM) at 80 C. The dust had a mass median aerodynamic diameter of about 0.8 micrometers A. The collection efficiencies of particles with aerodynamic diameters between 0.3 and 3 micrometers A were determined from size distribution data taken with cascade impactors. The efficiency data showed the venturi to be more efficient than predicted for particle sizes below 1 micrometer A. Particle mass augmentation by condensed water is a probable reason for the high efficiency for small particle collection. Diffusion battery data indicate the occurrence of some particle growth.

17. KEY WORDS AND DOCUMENT ANALYSIS

a. DESCRIPTORS	b. IDENTIFIERS/OPEN ENDED TERMS	c. COSATI Field/Group
Air Pollution	Air Pollution Control	13B 11G
Dust	Stationary Sources	07A
Scrubbers	Venturi Scrubbers	14B
Venturi Tubes	Kinpactor	08G,07B
Borax	Fusing Furnace	20M
Fusion (Melting) Furnaces		13A

18. DISTRIBUTION STATEMENT	19. SECURITY CLASS *(This Report)*	21. NO. OF PAGES
Unlimited	Unclassified	56
	20. SECURITY CLASS *(This page)*	22. PRICE
	Unclassified	

EPA Form 2220-1 (9-73)